Persistent Emission of Narrowband Ultraviolet-B Light upon Blue-Light Illumination

Siyi Yan,[1] Feng Liu,[1,*] Jiahua Zhang,[2] Xiao-jun Wang,[3] and Yichun Liu[1]

[1] *Key Laboratory for UV-Emitting Materials and Technology of Ministry of Education, Northeast Normal University, Changchun, 130024, China*

[2] *State Key Laboratory of Luminescence and Applications, Changchun Institute of Optics, Fine Mechanics and Physics, Chinese Academy of Sciences, Changchun, 130033, China*

[3] *Department of Physics, Georgia Southern University, Statesboro, Georgia 30460, USA*

(Received 6 July 2019; revised manuscript received 9 March 2020; accepted 30 March 2020; published 20 April 2020)

Ultraviolet luminescence holds potential for diverse applications. Further development of ultraviolet-luminescence technology, however, is hindered by the common but very inconvenient photoluminescence form. Here we create a form of ultraviolet emission—persistent luminescence in the narrowband ultraviolet-B (NB UVB) region (309–313 nm) upon illumination by a blue light-emitting diode. On this basis, we study the dynamic competition between an up-conversion charging excitation and a photostimulated detrapping upon illumination by the light-emitting diode. Such a competition mechanism, as well as the associated manipulation technique, appears to be generally applicable for many existing phosphors. As a proof of concept, we present an imaging demonstration, showing the potential of the NB-UVB persistent luminescence in the optical tagging field. This work can potentially revolutionize the ways for utilizing persistent luminescence, leading NB-UVB applications to another level.

DOI: 10.1103/PhysRevApplied.13.044051

I. INTRODUCTION

Ultraviolet light is present in sunlight as well as in artificial light, such as luminescence of phosphors. Ultraviolet light in the wavelength range from 309 to 313 nm is specifically referred to as narrowband ultraviolet-B (NB UVB) light, which has exhibited significant advantages in the medical field for treatment of skin diseases, including psoriasis and vitiligo [1,2]. While the market for NB-UVB technology is currently dominated by phototherapy lamps, the application potential of NB-UVB technology in other fields is often underestimated. For instance, NB UVB light has sufficient energy to induce light-responsive drug delivery [3,4]. Consequently, NB-UVB-emitting materials in the form of nanoparticles are expected to have important implications for light-mediated theranostics. Moreover, the general absence of ultraviolet spectral composition in an indoor-lighting environment enables the NB-UVB emission to be detected with zero background noise by an appropriate ultraviolet camera. According to such a visible-blind feature, optical tagging with NB-UVB-emitting materials can become an important technique to provide information for identification purposes in an indoor-lighting environment. Further development of NB-UVB technology is being hindered by the common but very inconvenient photoluminescence form. Thus, more diverse luminescence forms of NB-UVB phosphors are greatly needed to be explored.

Persistent luminescence as a special luminescence form has been extensively studied, first for visible persistent luminescence and recently for infrared persistent luminescence, and some visible persistent phosphors have gained commercial success and are being widely used as night-vision materials [5–9]. In contrast to the progress in visible and infrared persistent luminescence, research at the other end of the spectrum—the shorter-wavelength ultraviolet region is relatively lacking [10–14]. Taking into account the potential applications of NB UVB light, the investigation of NB-UVB persistent luminescence, as an alternative luminescence form, will be interesting and significant.

The practical NB-UVB luminescence generally originates from phosphors activated by trivalent gadolinium (Gd^{3+}) ions, which have no absorption in the visible-light region due to their unique energy-level structure and have no tendency to be oxidized or reduced in phosphor due to their stabilized $4f^7$ electron configuration. Compared with the extensive studies on the nonradiative role of Gd^{3+} in phosphors [15–18], few studies on Gd^{3+} emission have been reported [19–23], and these focus primarily on common photoluminescence upon real-time excitation by high-energy ionizing radiation or high-intensity coherent lasers. To achieve designable luminescence-performance

*fengliu@nenu.edu.cn

properties of Gd^{3+}-activated phosphor, it is essential to introduce a sensitizer ion, which should have a suitable high-lying state for efficient transfer of the excitation energy to Gd^{3+} ions [20–24]. As a sensitizer for Gd^{3+} emission, trivalent praseodymium (Pr^{3+}) ions are a good candidate [24] since Pr^{3+}-doped phosphors possess some fascinating optical properties [25–36]. Up-conversion luminescence from the high-lying $4f5d$ state of Pr^{3+} has been achieved upon excitation of the $^3P_0$ or $^1D_2$ level in some phosphors [27–31]. Moreover, electron transfer may occur between the delocalized state of Pr^{3+} and the trap state, since Pr^{3+} has a tendency to be oxidized in some solids [32–35]. Accordingly, we can envisage an up-conversion charging process [36–38] by combining the up-conversion and the electron-transfer characters of Pr^{3+}. Such a combination enables us to generate $4f5d \rightarrow 4f^2$ ultraviolet persistent luminescence after charging by visible-light illumination. As a consequence, persistent luminescence of Gd^{3+} in the NB UVB region is expected in appropriate Pr^{3+}-Gd^{3+}-codoped phosphors, in which the Pr^{3+} ion may absorb two-step-excitation energy to fill electron traps and then persistently transfers the stored energy to Gd^{3+}.

Here we develop a NB-UVB persistent phosphor, Pr^{3+}-Gd^{3+}-codoped $Lu_2Pr_{0.01}Gd_{0.99}Al_2Ga_3O_{12}$ (hereafter referred to as LuAGG:Pr,Gd). Persistent luminescence of 313 nm is successfully achieved in the phosphor after illumination by a widely available blue light-emitting diode (LED). Our spectroscopic results reveal that, depending on the blue-LED illumination at different power densities, the charging and discharging processes of the phosphor can be manipulated. Moreover, we demonstrate NB-UVB imaging based on the LuAGG:Pr,Gd phosphor, showing an optical tagging capability of the persistent luminescence in an indoor-lighting environment.

II. METHODS

A. Sample preparation

Phosphors with the general chemical formula of $Lu_{3-x-y}Pr_xGd_yAl_{5-z}Ga_zO_{12}$ ($x = 0.001$–0.1, $y = 0.05$–2.5, and $z = 1$–4) are synthesized by a solid-state-reaction method. Any combination of these variables can produce phosphor with NB-UVB persistent luminescence. In the study, we focus our discussion on the $Lu_2Pr_{0.01}Gd_{0.99}Al_2Ga_3O_{12}$ composition. Starting materials, including Lu_2O_3 (99.99%), Gd_2O_3 (99.999%), Al_2O_3 (99.99%), Ga_2O_3 (99.999%), and Pr_6O_{11} (99.99%), are mixed in stoichiometric proportions. After being finely ground in an agate mortar for 3 h, the mixture is pressed into a disk of 1.5-cm diameter with use of a 30-ton hydraulic press. The disk is then sintered for 3 h at 1300 °C in air to obtain the products.

B. Characterization

Luminescence excitation and emission spectra are measured with a Horiba FluoroMax Plus spectrofluorometer. The persistent-luminescence excitation spectrum is recorded after ceasing of illumination with monochromatic light from a built-in xenon arc lamp (included in the spectrofluorometer) [39]. The up-conversion excitation spectrum obtained by our monitoring the 313-nm emission is obtained by our exciting the phosphor with a pulsed laser (Continuum SureLite II Nd:YAG laser) with tunable wavelength from a Continuum SureLite optical parametric oscillator. Persistent-luminescence intensity (in the unit of microwatts per steradian per square meter) is evaluated with a Thorlabs PM320E optical power meter equipped with an ultraviolet extended power sensor (S130VC, Thorlabs). Thermoluminescence measurements are conducted with a modified version of an SL08-L TL reader (Guangzhou Rongfan Science and Technology Co. Ltd). The thermoluminescence curves are recorded for Gd^{3+} emission at 313 nm with a heating rate of 4 °C s^{-1}. Before each measurement, the phosphor is heat-treated at 450 °C to empty all the traps. A high-power blue LED (LUMINUS, CBT-90TE-B, peaking at 452 nm) equipped with a liquid cooling module is used as the primary excitation source. The phosphor is illuminated by means of the blue-LED light transmitted subsequently through a lens combination (Fig. S1 in Supplemental Material [40]). The illumination light path allows us to focus the LED beam into a spot with a diameter of 1 cm. The illumination power density presented in this study is defined as the beam power reaching the surface of the phosphor divided by the focused beam area. An Ofil Scalar camera (improved version), which is sensitive from 308 to 321 nm, is used for the visible-blind imaging. The imaging experiments are conducted in an indoor-lighting environment (the ambient light is from a Philips LED ceiling lamp). The image taken by the camera is an overlay image after superimposition of an ultraviolet image onto a visible image.

III. RESULTS AND DISCUSSION

A. Achievement of NB-UVB persistent luminescence

The LuAGG:Pr,Gd phosphor features persistent luminescence after various effective illuminations. For instance, upon ultraviolet illumination from a filtered xenon arc lamp, the phosphor exhibits 313-nm persistent luminescence, as well as visible persistent luminescence (see Fig. S2 in Supplemental Material [40]). The corresponding persistent-luminescence excitation spectrum, which is an indication of the delocalization energy for filling the traps [39], covers the range from 32 000 to 50 000 cm^{-1} [Fig. 1(a)]. Alternatively, persistent luminescence of the phosphor can also be achieved via an up-conversion charging process.

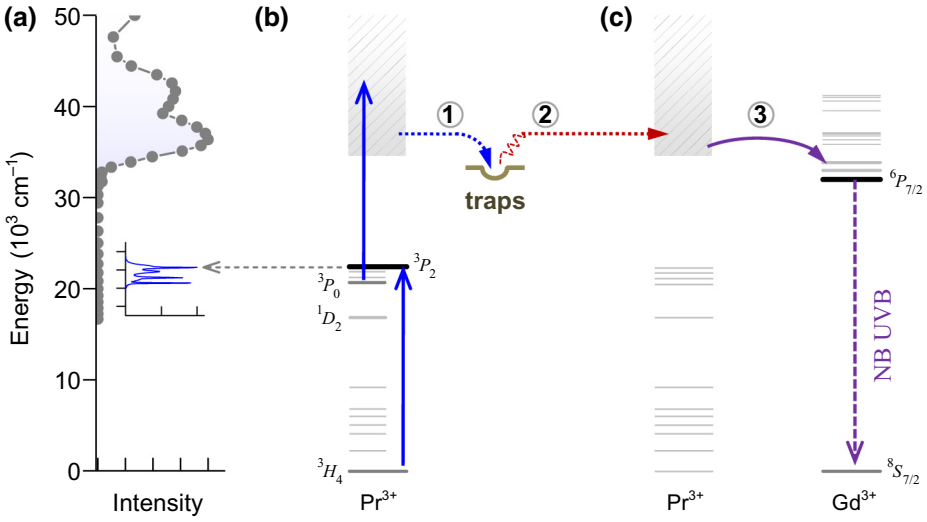

FIG. 1. Conceptual design of persistent luminescence in the NB UVB region upon blue-light illumination in LuAGG:Pr,Gd phosphor. (a) Persistent luminescence excitation spectrum for Gd^{3+} emission at room temperature. The inset shows an up-conversion excitation spectrum. (b) An up-conversion charging process upon intense blue-light illumination. The Pr^{3+} ion firstly absorbs two-step-excitation energy to fill electron traps (process 1), followed by gradually release of the traps at ambient temperature (process 2). The square frame in the high-energy region stands for the delocalized $4f5d$ state, whose energy scale corresponds to that of the persistent-luminescence excitation band in (a). (c) Persistent energy transfer from the excited Pr^{3+} ion to the Gd^{3+} ion (process 3), as well as the resulting persistent luminescence in the NB UVB spectral region.

A proposed scheme for the up-converted persistent luminescence in the NB UVB region is illustrated in Figs. 1(b) and 1(c). Under two-step up-conversion excitation with a blue-light illumination (see the up-conversion excitation spectrum presented in Fig. S3 in Supplemental Material [40]), the Pr^{3+} ion (sensitizer) is promoted to the $4f\ 5d$ state, which is associated with the delocalization property in the LuAGG:Pr,Gd phosphor at room temperature; see Fig. S2(c) in Supplemental Material [40]. The delocalized electron may be captured by traps (process 1) and subsequently released at ambient temperature (process 2), followed by the recombination with the ionized Pr^{3+}. Finally, the energy transfer from Pr^{3+} to Gd^{3+} accounts for the 313-nm emission (Fig. S4 in Supplemental Material [40]). Notably, during the up-conversion excitation, our spectroscopic investigation reveals that $^3P_0$ is a predominant intermediate state in the phosphor (Fig. S5 in Supplemental Material [40]).

The up-converted persistent luminescence in LuAGG:Pr,Gd is experimentally verified with use of a blue LED as the excitation source (power density 1 W cm^{-2}), whose output emission spectrum is presented in Fig. S3(b) in Supplemental Material [40]. When the LED illumination ceases, we record the persistent-luminescence spectra in the NB UVB region for different delay times from 5 to 60 min, as shown in Fig. 2(a). These emission spectra consist of a sharp peak at 313 nm, assigned to the Gd^{3+} $^6P_{7/2} \rightarrow {}^8S_{7/2}$ transition. The resulting persistent-luminescence intensities at delays of 5 and 60 min are estimated to be 70 and 9 μW sr^{-1} m^{-2}, respectively (Fig. S6 in Supplemental Material [40]).

To gain insight into the up-converted persistent luminescence in LuAGG:Pr,Gd, we conduct thermoluminescence measurements after illumination by the blue LED (1 W cm^{-2} illumination for 1 s). Figure 2(b) shows a typical thermoluminescence curve for the 313-nm emission, consisting of a dominating band with a maximum at 75 °C, as well as a long tail up to 380 °C. Our investigations suggest that, besides the depletion of traps with increasing temperature, the low quenching temperature of the emitting level also accounts for the absence of effective thermoluminescence at high temperature (see Fig. S7 in Supplemental Material [40]). That is, the low thermoluminescence intensity on the high-temperature side may stem from a combined contribution of the thermal depletion of traps and the thermal quenching of the emitting level.

B. Competition between up-conversion charging excitation and photostimulated detrapping

The nonlinear-excitation nature of the persistent luminescence in the LuAGG:Pr,Gd phosphor is verified by our measuring the dependence of thermoluminescence intensity on the LED illumination power density. We record the thermoluminescence curves for the 313-nm emission after blue-LED illumination at different incident power densities from 0.1 to 1.5 W cm^{-2}. These curves share a similar

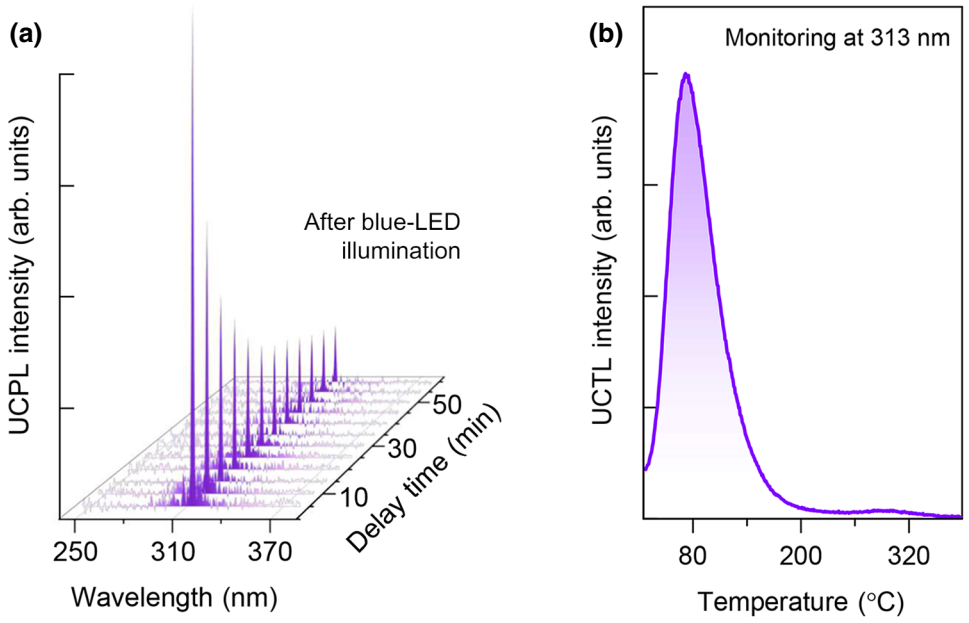

FIG. 2. Up-converted persistent luminescence (UCPL) and up-converted thermoluminescence (UCTL) of LuAGG:Pr,Gd recorded after ceasing of blue-LED illumination. (a) UCPL spectra recorded from 5 to 60 min after ceasing of the illumination (exposure duration 1 min). (b) UCTL curve for Gd^{3+} emission at 313 nm (exposure duration 1 s). The relatively low thermoluminescence intensity on the high-temperature side may stem from a combined contribution of thermal depletion of traps and thermal quenching of the emitting level (see the text for details). The LED illumination power density for both measurements is 1 W cm^{-2}.

spectral shape with various intensities (Fig. S8 in Supplemental Material [40]). Figure 3(a) depicts the integrated thermoluminescence intensity (I) as a function of the illumination power density (P) in a double-logarithmic plot. For illumination with an exposure duration of 1 s, the I-P curve is consistent with a quadratic relationship ($I \propto P^{1.86}$), providing strong evidence that two-photon excitation is involved in the up-conversion process. However, intriguingly, as the exposure duration is increased to 100 s, the I-P curve deviates from the quadratic relationship. Prior studies on the up-conversion charging phenomenon indicated that trap filling can be affected by photostimulation [36,37]. In such a charging mechanism, on the one hand, the traps can be filled through two-step photoionization of an activator ion (i.e., the electron trapping process). On the other hand, the external illumination can release some trapped electrons to the delocalized continuum state of the phosphor (i.e., the photostimulated-detrapping process). Consequently, the present results suggest that photostimulated detrapping may account for the deviation of the I-P quadratic relationship for long exposure durations.

We use a rate-equation approach to describe the effect of photostimulated detrapping on the up-conversion charging process, in which we assume that electron retrapping between different traps is negligible. Upon blue-LED excitation at power density P, as illustrated in Fig. 3(b), the rate equation during the illumination is

$$dN_2/dt = A_1N_1 - A_2N_2, \tag{1}$$

where N_1 is the population of the up-conversion delocalized state, N_2 is the electron population in the traps, A_1 is the trapping rate, and A_2 is the photostimulated-detrapping rate. Taking into account the features of up-conversion excitation [41] and photostimulated detrapping [42], we assume that $N_1 \propto P^n$ (n is the number of pump photons) and $A_2 \propto P$. If $A_1N_1 - A_2N_2 > 0$, integration of Eq. (1)

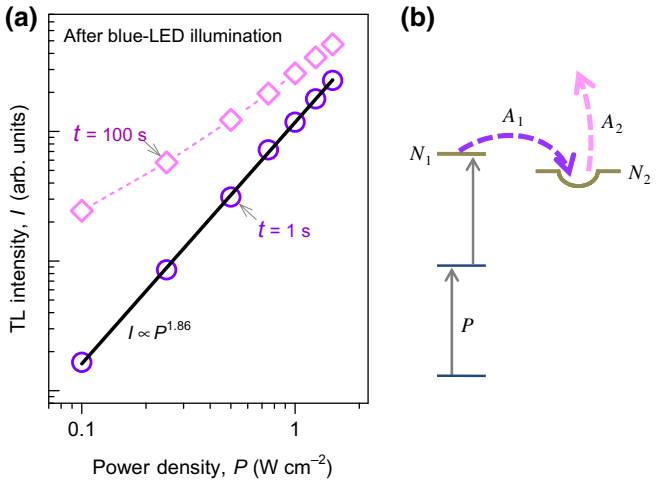

FIG. 3. Illumination-power-density dependence of thermoluminescence (TL) intensity of LuAGG:Pr,Gd for different exposure durations. (a) Integrated TL intensity (I) versus the power density (P) of the blue LED. The TL measurements are conducted by monitoring at 313 nm. The exposure durations (t) are 1 and 100 s, respectively. For $t = 1$ s, the I-P curve is consistent with a quadratic relationship, but the I-P curve deviates from the quadratic relationship upon illumination for $t = 100$ s. (b) Electron-trapping and photostimulated-detrapping processes upon illumination at power density P. N_1 is the population of the up-conversion delocalized state, N_2 is the electron population in the trap, A_1 is the trapping rate, and A_2 is the photostimulated-detrapping rate. Straight-line arrows and curved-line arrows represent the optical transitions and electron transfers, respectively.

gives

$$N_2 = C_1 P^{n-1} - (C_2/P)e^{-Pt}, \tag{2}$$

where C_1 and C_2 are positive constants. Accordingly, one can deduce that if electron trapping is dominant, the population in the trap increases with the illumination duration. In contrast, if $A_1N_1 - A_2N_2 < 0$, integration of (1) yields

$$N_2 = C_1 P^{n-1} + (C_2/P)e^{-Pt}. \tag{3}$$

This means that if photostimulated detrapping is dominant, the population in the traps will decrease with the illumination duration.

We further design an extended thermoluminescence measurement, as outlined in Fig. 4(a), to experimentally evaluate the competition between electron trapping and photostimulated detrapping in the LuAGG:Pr,Gd phosphor. We illuminate the phosphor using the blue LED with power densities of 1.5 and 0.1 W cm^{-2}, respectively, which are the maximum and minimum power densities presented in Fig. 3(a). Firstly, we illuminate the phosphor using 1.5 W cm^{-2} for 5 s to fill some of the traps (initial illumination mode). Subsequently, we illuminate the phosphor twice by combining the 5-s initial illumination and a secondary illumination, whose power density is fixed at 1.5 W cm^{-2} [high-power (HP) mode] or 0.1 W cm^{-2} [low-power (LP) mode]. As shown in Fig. 4(a), the HP mode starts in the time frame from 840 to 900 s and ends at 900 s after the initial illumination (i.e., the HP duration ranges from 60 to 0 s). The LP mode starts in the time frame from 0–900 s and also ends at 900 s (i.e., the LP duration ranges from 900 to 0 s). All the associated thermoluminescence measurements for the 313-nm emission start at 1000 s after the initial illumination (Fig. S9 in Supplemental Material [40]). In accordance with the description in Fig. 3(b), the HP and LP modes are expected to influence the thermoluminescence intensity in different ways (note that the integrated thermoluminescence intensity is an indication of the electron population in the traps [43]).

Figure 4(b) plots the integrated thermoluminescence intensities of the LuAGG:Pr,Gd phosphor versus the secondary exposure dose, which is equal to the power density multiplied by the exposure duration. The ascending curve shows that the thermoluminescence intensity increases with the HP illumination duration, indicating that the phosphor is being charged under the HP mode, as given in (2). In contrast, under the LP mode, the thermoluminescence intensity decreases with increasing illumination duration, as described in (3). We therefore conclude that the net population in the traps can be adjusted by use of the blue LED with different power densities. That is, the phosphor can be charged by a high-power illumination but discharged by a low-power illumination. The charging-discharging dynamics shown in Fig. 4 is intrinsic for the present up-converted persistent luminescence and does not

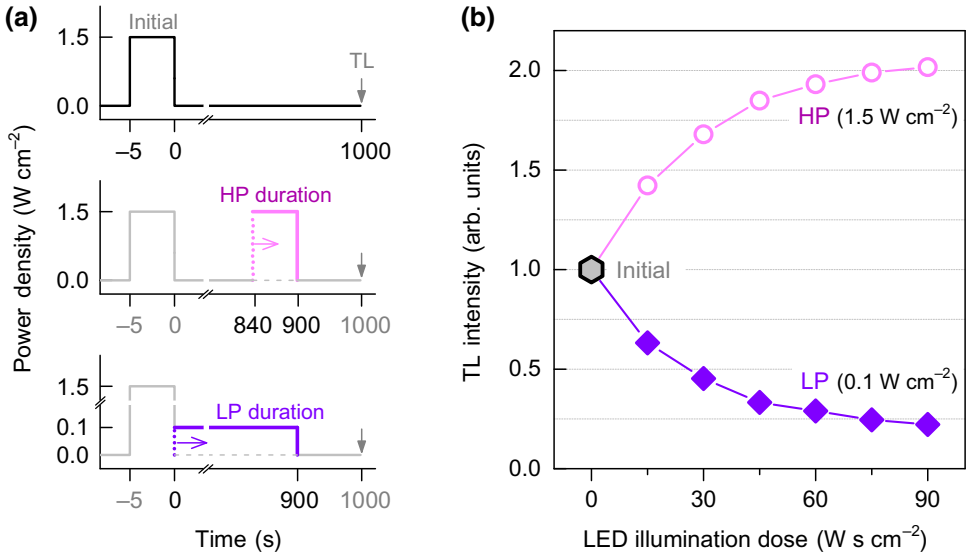

FIG. 4. Charging and discharging of LuAGG:Pr,Gd upon blue-LED illumination at different power densities. (a) Outline of the experiment. The phosphor is initially illuminated for 5 s at 1.5 W cm^{-2} to fill some of the traps (initial illumination mode). Subsequently, the phosphor is exposed to secondary illumination, whose power density is fixed at 1.5 W cm^{-2} (high power density, HP mode) or 0.1 W cm^{-2} (low power density, LP mode). In this study, the HP illumination starts in the time frame from 840 to 900 s with exposure durations of 10, 20, 30, 40, 50, and 60 s. The LP illumination starts in the time frame from 0 to 900 s with exposure durations of 150, 300, 450, 600, 750, and 900 s. Each secondary illumination ends at 900 s, and the associated thermoluminescence (TL) measurement starts at 1000 s. The TL measurements are conducted by monitoring at 313 nm. (b) Integrated TL intensity versus the secondary exposure dose, which is equal to the power density multiplied by the exposure duration.

work for the conventional persistent-luminescence process (Fig. S10 in Supplemental Material [40]).

Figure 4 also shows that the discharging process (LP mode, 0–900 s) is much slower than the charging process (HP mode, 0–60 s). Accordingly, we can deduce that for a sample with emptied traps, upon illumination with a short exposure duration (e.g., $t = 1$ s), the effect of photostimulated detrapping may be negligibly small. Thus, the net population in the traps is approximately proportional to the amount of delocalization electrons ($N_2 \propto P^n$). The result is consistent with the observation in Fig. 3(a), in which the integrated thermoluminescence intensity is approximately proportional to the square of the LED power density. Upon illumination with a long exposure duration (i.e., $t = 100$ s), the effect of photostimulated detrapping is relatively significant [$N_2 = C_1 P^{n-1} - (C_2/P)e^{-Pt}$], so the I-P function in Fig. 3(a) deviates from the quadratic relationship.

C. Tagging with NB-UVB persistent luminescence

The unique spectroscopic performances, involving persistent luminescence in the NB UVB region and up-conversion charging excitation upon blue-LED illumination, make the LuAGG:Pr,Gd phosphor a potential candidate for some interesting applications, such as a conceptual Band-Aid-type phototherapy solution (see Fig. S11 in Supplemental Material [40]) or visible-blind tagging. As an example, by taking advantage of the zero NB-UVB background of the indoor-lighting environment, we use an Ofil Scalar camera to demonstrate the capability of the phosphor for visible-blind tagging. Figure 5(a) gives the persistent-luminescence spectrum of the LuAGG:Pr,Gd phosphor recorded at 10 s after stoppage of the blue-LED illumination (incident power density 1 W cm^{-2}). Coincidentally, such emission fits well the spectral coverage of the Ofil Scalar camera, which is sensitive from 308 to 321 nm but insensitive to indoor ambient light [Fig. 5(a) and Fig. S12 in Supplemental Material [40]]. Figures 5(b) and 5(c) illustrate overlay images (superimposing NB-UVB images onto visible images), showing an activated LuAGG:Pr,Gd phosphor disk attached to the right shoulder of a person. The NB-UVB imaging is indicated by a red pattern, whose area is proportional to the emission intensity. Under LED illumination, the phosphor generates a NB-UVB-emitting spot (up-conversion luminescence), enabling clear imaging with the camera [Fig. 5(b)]. After ceasing of the LED illumination, as shown in Fig. 5(c), the phosphor disk exhibits NB-UVB persistent luminescence (delay time 10 s), indicating that the phosphor has been charged by the LED. Moreover, the manipulation of charging and discharging is also visually verified by an extended imaging experiment using the Ofil Scalar camera, as presented in Fig. S12 in Supplemental Material [40]. Such an imaging demonstration shows an advantage of the NB-UVB persistent luminescence in the optical tagging field

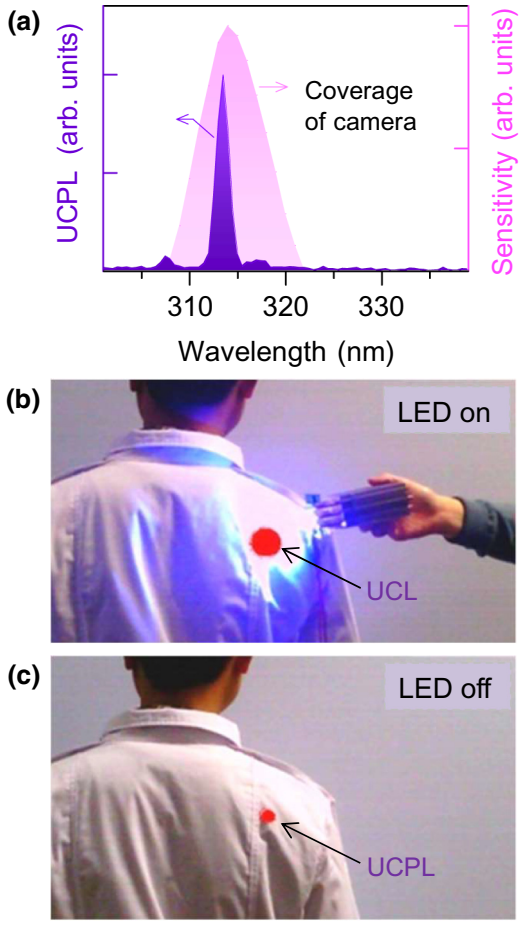

FIG. 5. Demonstration of a NB-UVB tag containing the LuAGG:Pr,Gd persistent phosphor for identification purposes in an indoor-lighting environment. (a) Persistent-luminescence spectrum of LuAGG:Pr,Gd phosphor recorded 10 s after ceasing of blue-LED illumination. The emission spectrum coincides well with the spectral coverage of the Ofil Scalar camera. (b) A person wearing a LuAGG:Pr,Gd phosphor disk, which is being illuminated by the LED. The NB-UVB imaging is indicated by a red pattern, whose area is proportional to the emission intensity. Under illumination with the LED, the phosphor disk generates NB-UVB up-conversion luminescence (UCL). (c) After ceasing of LED illumination (delay time 10 s), the phosphor disk keeps emitting NB UVB light, indicating that the phosphor has been charged through the up-conversion charging process by the LED. UCPL, up-converted persistent luminescence.

(notably, visible and near-infrared persistent luminescence cannot function as optical tagging in an indoor-lighting environment due to the ambient light noise). Accordingly, the present research provides a major step toward further development of optical tagging applications.

IV. CONCLUSIONS

We achieve NB-UVB persistent luminescence in LuAGG:Pr,Gd phosphor upon blue-LED illumination. Our investigations indicate that the net population in the traps

in the phosphor is dominated by competition between a nonlinear excitation and a photostimulated release of electrons from traps. The competitive process can be manipulated by use of the same blue LED with different power densities. In addition, besides the blue-LED illumination, the persistent luminescence phenomenon in the LuAGG:Pr,Gd phosphor is also observed with use of various blue lasers, such as 450- and 459-nm laser diodes and 473- and 488-nm solid-state lasers (Fig. S13 in Supplemental Material [40]). The achievement and manipulation of up-converted persistent luminescence in the NB UVB region offer a unique opportunity to use this special optical phenomenon for many alternative applications where the NB-UVB emission is preferred and high-energy ultraviolet or x-ray excitation is inconvenient.

ACKNOWLEDGMENTS

The work was supported by the National Natural Science Foundation of China (Grants No. 11774046, No. 11874055, and No. 51732003) and the Department of Science and Technology of Jilin Province (Grant No. 20180414082GH).

[1] S. H. Ibbotson, D. Bilsland, N. H. Cox, R. S. Dawe, B. Diffey, C. Edwards, P. M. Farr, J. Ferguson, G. Hart, J. Hawk, J. Lloyd, C. Martin, H. Moseley, K. McKenna, L. E. Rhodes, and D. K. Taylor, An update and guidance on narrowband ultraviolet B phototherapy: A British photodermatology group workshop report, Br. J. Dermatol. **151**, 283 (2004).

[2] M. Berneburg, M. Rocken, and F. Benedix, Phototherapy with narrowband vs broadband UVB, Acta Derm. Venereol. **85**, 98 (2005).

[3] A. Barhoumi, Q. Liu, and D. S. Kohane, Ultraviolet light-mediated drug delivery: Principles, applications, and challenges, J. Control. Release **219**, 31 (2015).

[4] X. Ai, J. Mu, and B. Xing, Recent advances of light-mediated theranostics, Theranostics **6**, 2439 (2016).

[5] T. Matsuzawa, Y. Aoki, N. Takeuchi, and Y. Murayama, A new long phosphorescent phosphor with high brightness, $SrAl_2O_4$: Eu^{2+},Dy^{3+}, J. Electrochem. Soc. **143**, 2670 (1996).

[6] P. F. Smet, K. Van den Eeckhout, O. Q. De Clercq, and D. Poelman, in *Handbook on the Physics and Chemistry of Rare Earths*, edited by J. C. Bunzli, V. K. Pecharsky (Elsevier, Amsterdam, 2015), Vol. 48.

[7] Y. Li, M. Gecevicius, and J. Qiu, Long persistent phosphor − from fundamentals to applications, Chem. Soc. Rev. **45**, 2090 (2016).

[8] J. Xu and S. Tanabe, Persistent luminescence instead of phosphorescence: History, mechanism, and perspective, J. Lumin. **205**, 581 (2019).

[9] Y. J. Liang, F. Liu, Y. F. Chen, X. J. Wang, K. N. Sun, and Z. W. Pan, New function of the Yb^{3+} ion as an efficient emitter of persistent luminescence in the short-wave infrared, Light Sci. Appl. **5**, e16124 (2016).

[10] Y. J. Liang, F. Liu, Y. F. Chen, K. N. Sun, and Z. W. Pan, Long persistent luminescence in the ultraviolet in Pb^{2+}-doped $Sr_2MgGe_2O_7$ persistent phosphor, Dalton Trans. **45**, 1322 (2016).

[11] W. Wang, Z. Sun, X. He, Y. Wei, Z. Zou, J. Zhang, Z. Wang, Z. Zhang, and Y. Wang, How to design ultraviolet emitting persistent materials for potential multifunctional applications: A living example of a $NaLuGeO_4$:Bi^{3+}, Eu^{3+} phosphor, J. Mater. Chem. C **5**, 4310 (2017).

[12] Y. M. Yang, Z. Y. Li, J. Y. Zhang, Y. Lu, S. Q. Guo, Q. Zhao, X. Wang, Z. J. Yong, H. Li, J. P. Ma, Y. Kuroiwa, C. Moriyoshi, L. L. Hu, L. Y. Zhang, L. R. Zheng, and H. T. Sun, X-ray-activated long persistent phosphors featuring strong UVC afterglow emissions, Light Sci. Appl. **7**, 88 (2018).

[13] P. X. Xiong and M. Y. Peng, Recent advances in ultraviolet persistent phosphors, Opt. Mater. X **2**, 100022 (2019).

[14] J. Shi, X. Sun, S. Zheng, X. Fu, Y. Yang, J. Wang, and H. Zhang, Super-long persistent luminescence in the ultraviolet A region from a Bi^{3+}-doped $LiYGeO_4$ phosphor, Adv. Opt. Mater. **7**, 1900526 (2019).

[15] Y. Liu, D. Tu, H. Zhu, R. Li, W. Luo, and X. Chen, A strategy to achieve efficient dual-mode luminescence of Eu^3+ in lanthanides doped multifunctional $NaGdF_4$ nanocrystals, Adv. Mater. **22**, 3266 (2010).

[16] F. Wang, R. Deng, J. Wang, Q. Wang, Y. Han, H. Zhu, X. Chen, and X. Liu, Tuning upconversion through energy migration in core-shell nanoparticles, Nat. Mater. **10**, 968 (2011).

[17] B. Zhou, B. Shi, D. Jin, and X. Liu, Controlling upconversion nanocrystals for emerging applications, Nat. Nanotech. **10**, 924 (2015).

[18] R. T. Wegh, H. Donker, K. D. Oskam, and A. Meijerink, Visible quantum cutting in $LiGdF_4$:Eu^{3+} through downconversion, Science **283**, 663 (1999).

[19] L. H. Brixner, M. K. Crawford, G. Hyatt, W. T. Carnall, and G. Blasse, Structure and luminescence of the $La_{1-x}Gd_xF_3$ system, J. Electrochem. Soc. **138**, 313 (1991).

[20] S. Espinoza, T. Juestel, and M. Haase, Colloidal $LaPO_4$:Gd^{3+} nanocrystals: X-ray induced single line UV emission, Nanoscale **10**, 22533 (2018).

[21] B. Zhou, J. Huang, L. Yan, X. Liu, N. Song, L. Tao, and Q. Zhang, Probing energy migration through precise control of interfacial energy transfer in nanostructure, Adv. Mater. **31**, 1806308 (2019).(2019).

[22] C. Cao, W. Qin, J. Zhang, Y. Wang, P. Zhu, G. Wei, G. Wang, R. Kim, and L. Wang, Ultraviolet upconversion emissions of Gd^{3+}, Opt. Lett. **33**, 857 (2008).

[23] A. R. Gharavi and G. L. McPherson, Ultraviolet emissions from Gd^{3+} ions excited by energy transfer from pairs of photoexcited Er^{3+} ions: Upconversion luminescence from $CsMgCl_3$ crystals doped with Gd^{3+} and Er^{3+}, J. Opt. Soc. Am. B **11**, 913 (1994).

[24] A. J. de Vries and G. Blasse, On the possibility to sensitize Gd^{3+} luminescence by the Pr^{3+}ion, Mater. Res. Bull. **21**, 683 (1986).

[25] F. Liu and X. J. Wang, Effects of non-4f states on Pr^{3+} luminescence in phosphors, Chin. J. Lumin. **38**, 1 (2017).

[26] X. Qin, X. Liu, W. Huang, M. Bettineli, and X. Liu, Lanthanide-activated phosphors based on 4f-5d optical transitions: Theoretical and experimental aspects, Chem. Rev. **117**, 4488 (2017).

[27] Y. M. Cheung and S. K. Gayen, Excited-state absorption in Pr^{3+}:$Y_3Al_5O_{12}$, Phys. Rev. B **49**, 14827 (1994).

[28] X. J. Wang, S. Huang, L. Lu, W. M. Yen, A. M. Srivastava, and A. A. Setlur, Measurement of quantum efficiency in Pr^{3+}-doped $CaAl_4O_7$ and $SrAl_4O_7$ crystals, Appl. Phys. Lett. **79**, 2160 (2001).

[29] C. Hu, C. Sun, J. Li, Z. Li, H. Zhang, and Z. Jiang, Visible-to-ultraviolet upconversion in Pr^{3+}:Y_2SiO_5 crystals, Chem. Phys. **325**, 563 (2006).

[30] E. L. Cates and J. H. Kim, Upconversion under polychromatic excitation: Y_2SiO_5:Pr^{3+},Li^+ converts violet, cyan, green, and yellow light into UVC, Opt. Mater. **35**, 2347 (2013).

[31] V. Gorieva, S. Korableva, and V. Semashko, Excited-state absorption spectra of Pr^{3+} ions doped into $LiY_{0.3}Lu_{0.7}F_4$ mixed crystal, Opt. Mater. Express **6**, 1146 (2016).

[32] G. Wittmann and R. M. Macfarlane, Photon-gated photoconductivity of Pr^{3+} YAG, Opt. Lett. **2**, 426 (1996).

[33] E. van der Kolk, P. Dorenbos, C. W. E. van Eijk, S. A. Basun, G. F. Imbusch, and W. M. Yen, 5d electron delocalization of Ce^{3+} and Pr^{3+} in Y_2SiO_5 and Lu_2SiO_5, Phys. Rev. B **71**, 165120 (2005).

[34] N. Kristianpoller, D. Weiss, N. Khaidukov, V. Makhov, and R. Chen, Thermoluminescence of some Pr^{3+} doped fluoride crystals, Radiat. Meas. **43**, 245 (2008).

[35] J. Ueda, A. Meijerink, P. Dorenbos, A. J. J. Bos, and S. Tanabe, Thermal ionization and thermally activated crossover quenching processes for 5d−4f luminescence in $Y_3Al_{5-x}Ga_xO_{12}$:Pr^{3+}, Phys. Rev. B **95**, 014303 (2017).

[36] Y. Chen, F. Liu, Y. Liang, X. Wang, J. Bi, X. J. Wang, and Z. Pan, A new up-conversion charging concept for effectively charging persistent phosphors using low-energy visible-light laser diodes, J. Mater. Chem. C **6**, 8003 (2018).

[37] F. Liu, Y. Liang, and Z. Pan, Detection of Up-Converted Persistent Luminescence in the Near Infrared Emitted by the $Zn_3Ga_2GeO_8$:Cr^{3+},Yb^{3+},Er^{3+} Phosphor, Phys. Rev. Lett. **113**, 177401 (2014).

[38] F. Liu, Y. Chen, Y. Liang, and Z. Pan, Phonon-assisted upconversion charging in $Zn_3Ga_2GeO_8$:Cr^{3+} near-infrared persistent phosphor, Opt. Lett. **41**, 954 (2016).

[39] Z. Pan, Y. Lu, and F. Liu, Sunlight-activated long-persistent luminescence in the near-infrared from Cr^{3+}-doped zinc gallogermanates, Nat. Mater. **11**, 58 (2012).

[40] See Supplemental Material at http://link.aps.org/supplemental/10.1103/PhysRevApplied.13.044051 for Figs. S1–S13.

[41] M. Pollnau, D. R. Gamelin, S. R. Luthi, H. U. Gudel, and M. P. Hehlen, Power dependence of upconversion luminescence in lanthanide and transition-metal-ion systems, Phys. Rev. B **61**, 3337 (2000).

[42] C. Tydtgat, K. W. Meert, D. Poelman, and P. F. Smet, Optically stimulated detrapping during charging of persistent phosphors, Opt. Mater. Express **6**, 844 (2016).

[43] K. Van den Eeckhout, A. J. J. Bos, D. Poelman, and P. F. Smet, Revealing trap depth distributions in persistent phosphors, Phys. Rev. B **87**, 045126 (2013).